JOURNAL OF GUIDANCE, CONTROL, AND DYNAMICS
Vol. 23, No. 4, July–August 2000

Linear Time-Varying Approach to Satellite Attitude Control Using Only Electromagnetic Actuation

Rafał Wiśniewski
Aalborg University, DK-9220 Aalborg Ø, Denmark

Recently, small satellite missions have gained considerable interest due to low-cost launch opportunities and technological improvement of microelectronics. Required pointing accuracy of small, inexpensive satellites is often relatively loose, within a couple of degrees. Application of cheap, lightweight, and power efficient actuators is therefore crucial and viable. Linear attitude control strategies for a low-Earth-orbit satellite actuated by a set of mutually perpendicular electromagnetic coils are discussed. The principle is to use the interaction between the Earth's magnetic field and the magnetic field generated by the coils. A key challenge is that the mechanical torque can only be produced in a plane perpendicular to the local geomagnetic field vector; therefore, the satellite is not controllable when considered at fixed time. Availability of design methods for time-varying systems is limited; nevertheless, a solution of the periodic Riccati equation gives an excellent framework for development and analysis of magnetic attitude control algorithms. An observation that the geomagnetic field changes approximately periodically when a satellite is on a near-polar orbit is used. Three types of attitude controllers are proposed: an infinite horizon, a finite horizon, and a constant gain controller. Their performance is evaluated and compared in the simulation study of the realistic environment.

Introduction

THE work is motivated by the Ørsted satellite mission. The Ørsted satellite is a 60-kg auxiliary payload launched by a Boeing-Delta II launch vehicle in February 1999 into a 654 × 871 km orbit with a 96-deg inclination. The purpose of the Ørsted satellite is to conduct research on the magnetic field of the Earth. When the satellite is firmly stabilized and ground contact is established, an 8-m-long gravity gradient boom is deployed. The boom carries scientific instruments that must be displaced from the electromagnetic disturbances present in the main body of the satellite. The requirements on pointing accuracy are relatively loose: pitch, roll, and yaw must be kept within 10 deg.

A concept for attitude control has been proposed based on magnetorquers as the only active torque source. The interaction between the external magnetic field of the Earth and the magnetic field generated in the magnetorquers produces a mechanical torque, which is used to correct the attitude. Magnetic control systems are comparatively lightweight, require low power, and are inexpensive; however, they can only be applied for satellites on relatively high inclined orbits. The Ørsted's coils are mounted in the x, y, and z faces of the main body. The maximum magnetic moment generated by the magnetorquers is 20 Am^2, which corresponds to the mechanical torque of 0.6×10^{-3} Nm above the equator and 1.2×10^{-3} Nm above the poles. After boom deployment the nominal operation phase controller is activated. The control task is to stabilize the satellite in three axes with its boom pointing outwards from the Earth. Formally, a coordinate system fixed in the satellite structure shall coincide with a reference coordinate system fixed in orbit.

The attitude control algorithms rely on both the satellite angular velocity and the attitude (quaternion) availability. This information is provided by the attitude determination algorithm based on a combination of accessible sensor inputs in an extended Kalman filter.[1] There are basically three sensors available for attitude determination: a triaxial fluxgate magnetometer, a star camera, and a wide-angle coarse sun sensor. Nominally, the attitude estimator uses the camera, however, in the case of contingency the magnetometer or a combination of the magnetometer and the sun sensor data are utilized.

There is extensive literature covering satellite attitude control design. However, most of the algorithms presented assume application of reaction wheels and/or thrusters for three-axis stabilization. The magnetic attitude control has the significant limitation that the control torque is always perpendicular to the local geomagnetic field vector. Therefore, the magnetic torquing was mainly used for unloading the excess angular momentum of a spacecraft reaction wheel control system in the presence of secular environmental torques.[2]

The available literature on magnetorquing for three-axis stabilization of satellites includes the work of Cavallo et al.[3] A globally stabilizing controller was developed for a configuration with two magnetic coils and a reaction wheel. Three-axis stabilization of a satellite without appendages with use of magnetic torquing only was treated by Wisniewski.[4] A sliding control law was provided and shown to stabilize a tumbling satellite. A novel approach based on a rule-based fuzzy controller was proposed by Steyn.[5] Still another approach for three-axis magnetic stabilization of a low-Earth near-polar orbit satellite based on Lyapunov theory was addressed by

Rafael Wiśniewski was born in Szczecin, Poland in 1968. He received his M.S. degree in engineering from Technical University of Szczecin, Poland, in 1992 and Ph.D. degree in electrical engineering from Aalborg University, Denmark, in 1997. He is currently an Associate Professor at the Department of Control Engineering, Aalborg University. His research interests are in nonlinear control theory, periodic systems, attitude control, and estimation. raf@control.auc.dk.

Received 10 June 1997; presented as Paper A97-37029 at the AIAA Guidance, Navigation, and Control Conference, New Orleans, LA, 11–13 August 1997; revision received 12 November 1997; accepted for publication 23 December 1999.

Wisniewski and Blanke,[6] where a global stabilizing magnetic controller was derived.

A number of internationally published papers dealing with magnetic attitude control can be extended to these addressing a linear control problem. Arduini and Baiocco[7] proposed a control law in which the desired control torque was defined first, and then the actual magnetic generated control torque was derived. Another concept cited in the literature was based on an idea of designing a magnetic controller for the system with averaged parameters. This design strategy was used both for bias momentum satellites[2,8,9] and three-axis control.[10]

This paper is an extension of the earlier work on the linear methods for magnetic attitude control. The system adopted here is chosen to be time varying because in linear time-invariant settings the satellite is only controllable in two axes, and the full controllability is first reached by considering time dependency of the geomagnetic field. An observation that the geomagnetic field changes approximately periodically when a satellite is on a near-Earth orbit is crucial for the development of magnetic control algorithms presented in this work because the design schemes are based on a solution of the periodic Riccati equation.

The first part of this study addresses a linearization technique for satellite motion. It is shown that a satellite on a near-polar orbit actuated by a set of perpendicular magnetorquers may be considered a periodic system. In the subsequent sections, three types of controllers are designed: an infinite horizon, a finite horizon, and a constant gain controller. The infinite and finite horizon controllers are stable by construction. On the contrary, stability of the constant gain control is further analyzed with use of Floquet theory. Performance of the three control laws is compared in the simulation study of the realistic environment.

Satellite Linear Model

The satellite considered in this study is modeled as a rigid body in the Earth's gravitational field influenced by the aerodynamic drag torque and the control torque generated by the magnetorquers. The attitude is parameterized by the unit quaternion providing a singularity-free representation of the kinematics. In this paper, only a satellite linear model will be investigated.

It has already been mentioned that the control torque, $\boldsymbol{N}_{\text{ctrl}}$, of the magnetic actuated satellite always lies perpendicular to the geomagnetic field vector $\boldsymbol{b}$. Furthermore, a magnetic moment $\boldsymbol{m}$ generated in the direction parallel to the local geomagnetic field has no influence on the satellite motion. This can be explained by the following equality

$$\boldsymbol{N}_{\text{ctrl}} = (\boldsymbol{m}_{\parallel} + \boldsymbol{m}_{\perp}) \times \boldsymbol{b} = \boldsymbol{m}_{\perp} \times \boldsymbol{b} \tag{1}$$

where $\boldsymbol{m}_{\parallel}$ is the component of the magnetic moment $\boldsymbol{m}$, parallel to $\boldsymbol{b}$, whereas $\boldsymbol{m}_{\perp}$ is perpendicular to the local geomagnetic field.

Concluding, the necessary condition for power optimality of a control law is that the magnetic moment lies on a plane perpendicular to the geomagnetic field vector.

Consider the following mapping:

$$\tilde{\boldsymbol{m}} \mapsto \boldsymbol{m} : \boldsymbol{m} = \tilde{\boldsymbol{m}} \times \boldsymbol{b} \tag{2}$$

where $\tilde{\boldsymbol{m}}$ represents a new control signal for the satellite. Now, the magnetic moment $\boldsymbol{m}$ is exactly perpendicular to the local geomagnetic field vector and the control theory for a system with unconstrained input $\tilde{\boldsymbol{m}}$ can be applied. The direction of the signal vector $\tilde{\boldsymbol{m}}$ (contrary to $\boldsymbol{m}$) can be chosen arbitrarily by the controller.

The linear model of the satellite motion is given in terms of the angular velocity and the first three components of the attitude quaternion. Linearization of the angular velocity is commonplace and based on the first-order extension of the Taylor series. Linearization of the attitude quaternion is quite different. The unit quaternion forms a group with quaternion multiplication as a binary operation, thus, multiplicative transformation is needed to describe successive rotations. Consider two rotations, the first one from an orbit fixed coordinate system (OCS) to a reference coordinate system (RCS) (this transformation is used for the yaw reference) and the second from RCS to a satellite fixed coordinate system (SCS):

$$^{S}_{O}\boldsymbol{q} = {}^{R}_{O}\boldsymbol{q}\,{}^{S}_{R}\boldsymbol{q} \tag{3}$$

where ${}^{S}_{R}\boldsymbol{q}$, ${}^{R}_{O}\boldsymbol{q}$, and ${}^{S}_{O}\boldsymbol{q}$ mean the quaternion mapping from RCS to SCS, the quaternion from OCS to RCS, and the quaternion from OCS to SCS, respectively. Now ${}^{S}_{R}\boldsymbol{q}$ can be considered as a small perturbation from the reference $[0\ \ 0\ \ 0\ \ 1]^T$. According to the definition of an attitude quaternion[11]

$${}^{S}_{R}\boldsymbol{q} = [e_1 \sin(\delta\phi/2) \quad e_2 \sin(\delta\phi/2) \quad e_3 \sin(\delta\phi/2) \quad \cos(\delta\phi/2)]^T \tag{4}$$

and for small $\delta\phi$

$${}^{S}_{R}\boldsymbol{q} \approx [\delta q_1 \quad \delta q_2 \quad \delta q_3 \quad 1]^T \equiv \begin{pmatrix} \boldsymbol{\delta q} \\ 1 \end{pmatrix} \tag{5}$$

For the sake of clarity, OCS and RCS are assumed in the following to coincide, and the system is linearized about the OCS. The y axis of RCS (OCS) is the positive normal to the orbit plane, and the z axis is zenith pointing. As the result, the linearized equation of motion is

$$\frac{\mathrm{d}}{\mathrm{d}t}\begin{pmatrix} \boldsymbol{\delta\Omega} \\ \boldsymbol{\delta q} \end{pmatrix} = \boldsymbol{A}\begin{pmatrix} \boldsymbol{\delta\Omega} \\ \boldsymbol{\delta q} \end{pmatrix} + \boldsymbol{B}(t)^{c}\tilde{\boldsymbol{m}} \tag{6}$$

where

$$\boldsymbol{A} = \begin{bmatrix} 0 & 0 & -\sigma_x\omega_o & -6\omega_o^2\sigma_x & 0 & 0 \\ 0 & 0 & 0 & 0 & 6\omega_o^2\sigma_y & 0 \\ -\omega_o\sigma_z & 0 & 0 & 0 & 0 & 0 \\ \frac{1}{2} & 0 & 0 & 0 & 0 & \omega_o \\ 0 & \frac{1}{2} & 0 & 0 & 0 & 0 \\ 0 & 0 & \frac{1}{2} & -\omega_o & 0 & 0 \end{bmatrix}$$

$$\sigma_x = \frac{I_y - I_z}{I_x}, \qquad \sigma_y = \frac{I_z - I_x}{I_y}, \qquad \sigma_z = \frac{I_x - I_y}{I_z}$$

$$\boldsymbol{B}(t) = \begin{bmatrix} \boldsymbol{I}^{-1}\begin{bmatrix} -b_y^2(t) - b_z^2(t) & b_x(t)b_y(t) & b_x(t)b_z(t) \\ b_x(t)b_y(t) & -b_x(t)^2 - b_z(t)^2 & b_y(t)b_z(t) \\ b_x(t)b_z(t) & b_y(t)b_z(t) & -b_x(t)^2 - b_y(t)^2 \end{bmatrix} \\ \begin{bmatrix} 0 & 0 & 0 \\ 0 & 0 & 0 \\ 0 & 0 & 0 \end{bmatrix} \end{bmatrix}$$

where ω_o is the orbital rate and I_x, I_y, and I_z are components on the diagonal of the inertia tensor $\boldsymbol{I}$ (the principal moments of inertia). The matrix $\boldsymbol{B}(t)$ comes from the double cross product operation $-\boldsymbol{b}(t) \times [\boldsymbol{b}(t) \times]$ divided by $\boldsymbol{I}$. The upper-left 3×3 submatrix of $\boldsymbol{A}$ is due to Euler coupling, the submatrix in the upper-right corner arises from the gravity gradient, and the lower part of the matrix $\boldsymbol{A}$ is the linearized kinematics.

Based on the mathematical model provided in this section, linear attitude control concepts will be developed. Three controllers will be proposed: an infinite horizon, a finite horizon, and a constant gain controller.

Infinite Horizon Periodic Controller

The geomagnetic field is essentially that of a magnetic dipole with the largest anomalies over Brazil and Siberia. The geomagnetic field in RCS has large x and z components, whereas the y component, perpendicular to the orbital plane, is comparatively small. The rotation of the Earth is visible via fluctuations of the y component of the geomagnetic field with a 24-h period (Fig. 1). The following observation is used for the design of an attitude controller: the magnetic field of the Earth on a near-polar orbit is approximately periodic with a period $T = 2\pi/\omega_0$.

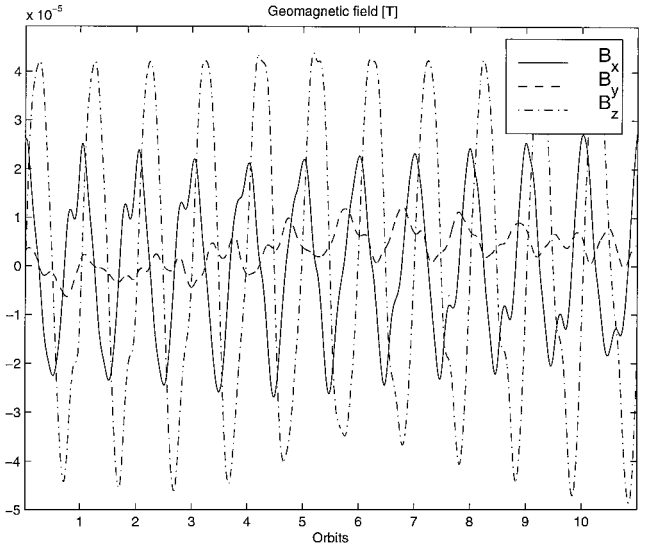

Fig. 1 Geomagnetic field vector in RCS propagated by 10th-order spherical harmonic model during 24 h in February 1999.

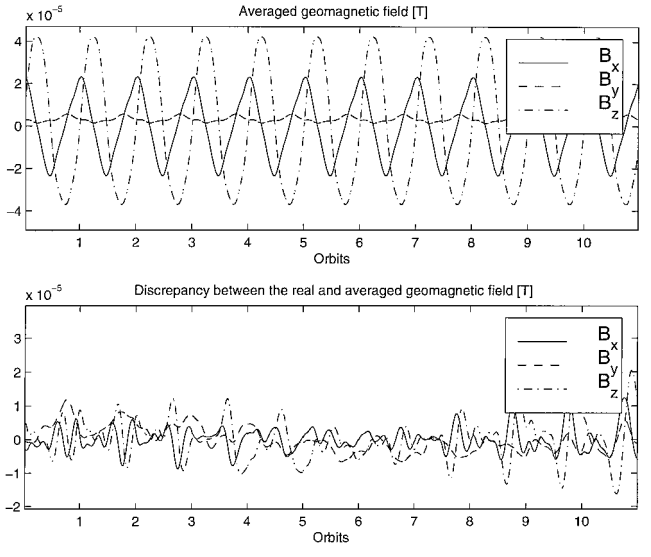

Fig. 2 Averaged geomagnetic field vector in RCS and discrepancy between the real field and its ideally periodic counterpart.

Because of the periodic nature of the geomagnetic field, the linearized model of the satellite can be considered periodic. It is, however, necessary to find an ideally periodic counterpart to the real magnetic field of the Earth as seen from RCS. This is done by averaging the geomagnetic field over a time interval corresponding to a common period for the satellite revolution about the Earth and the Earth's own rotation. This interval for the Ørsted satellite conforms to $N = 144$ orbits. Furthermore, the geomagnetic field is parameterized by the mean anomaly M because the geomagnetic field and the mean anomaly have the common period T,

$$\boldsymbol{b}_{\mathrm{av}}(M) = \frac{1}{N}\sum_{i=1}^{N}\boldsymbol{b}(M + iT) \tag{7}$$

An averaged $\boldsymbol{B}$-field vector $\boldsymbol{b}_{\mathrm{av}}[M(t)]$ is depicted in Fig. 2. Now the resultant linear periodic system is

$$\frac{\mathrm{d}}{\mathrm{d}t}\begin{pmatrix}\delta\boldsymbol{\Omega}\\ \delta\boldsymbol{q}\end{pmatrix} = \boldsymbol{A}\begin{pmatrix}\delta\boldsymbol{\Omega}\\ \delta\boldsymbol{q}\end{pmatrix} + \hat{\boldsymbol{B}}(M)\tilde{\boldsymbol{m}} \tag{8}$$

where $\hat{\boldsymbol{B}}(M)$ is given in Eq. (6) after substituting the symbol $\boldsymbol{B}(t)$ for $\hat{\boldsymbol{B}}(M)$ and the components of the vector $\boldsymbol{b}(t)$ for the components of $\boldsymbol{b}_{\mathrm{av}}(M)$. The difference between the time-varying matrix $\boldsymbol{B}(t)$ and the ideal periodic counterpart $\hat{\boldsymbol{B}}[M(t)]$ used for the controller design is considered as an additional external disturbance torque acting on the satellite. In the next subsection the problem of infinite horizon periodic control will be addressed.

Control Synthesis

The gain matrix for the infinite horizon controller is calculated from the periodic equilibrium of a certain Riccati equation whose coefficient matrices are periodic. A matrix $\boldsymbol{U}(t)$ will be called T periodic if $\boldsymbol{U}(t+T) = \boldsymbol{U}(t)$. In the most general settings, the periodic Riccati equation is given by

$$-\dot{\boldsymbol{P}}(t) = \boldsymbol{P}(t)\tilde{\boldsymbol{A}}(t) + \tilde{\boldsymbol{A}}^T(t)\boldsymbol{P}(t) - \boldsymbol{P}(t)\boldsymbol{B}(t)\boldsymbol{B}^T(t)\boldsymbol{P}(t) + \tilde{\boldsymbol{C}}^T(t)\tilde{\boldsymbol{C}}(t) \tag{9}$$

where the matrices $\tilde{\boldsymbol{A}}(t)$, $\boldsymbol{B}(t)$, and $\tilde{\boldsymbol{C}}(t)$ are T periodic. The properties of the periodic Riccati equation in many cases correspond to ones of the algebraic Riccati equation. It is well known that stabilizability and observability of a dynamic system determine solvability of the algebraic Riccati equation. Similar results are valid for the periodic Riccati equation.[12]

Theorem 1: There exists a stabilizing symmetric periodic solution $\boldsymbol{P}(t)$ to the Riccati equation (9) if and only if $[\tilde{\boldsymbol{A}}(t), \boldsymbol{B}(t)]$ is stabilizable and no unit-modulus characteristic multipliers of $\tilde{\boldsymbol{A}}(t)$ are $[\tilde{\boldsymbol{A}}(t), \tilde{\boldsymbol{C}}(t)]$ unobservable.

Having formulated the theorem on solvability of a periodic Riccati equation, the general infinite horizon control problem can be expressed. Let a dynamic system be described by

$$\dot{\boldsymbol{x}}(t) = \boldsymbol{A}(t)\boldsymbol{x}(t) + \boldsymbol{B}(t)\boldsymbol{u}(t), \qquad \boldsymbol{z}(t) = \boldsymbol{C}(t)\boldsymbol{x}(t) + \boldsymbol{D}(t)\boldsymbol{u}(t) \tag{10}$$

where the matrices $\boldsymbol{A}(t)$, $\boldsymbol{B}(t)$, $\boldsymbol{C}(t)$, and $\boldsymbol{D}(t)$ are T periodic. The second equation in Eq. (10) is added artificially, and it serves as a specification of the control objective in the time domain. It is assumed in this description that the full state information is available. The objective of the design is to find a controller that makes the L_2 norm of the output signal $\boldsymbol{z}(t)$ minimal.

To solve this problem, suppose that the periodic system (10) fulfills the following assumptions:

1) $\boldsymbol{D}(t)$ has full column rank with $[\boldsymbol{D}(t)\ \ \boldsymbol{D}_\perp(t)]$ being unitary.

2) The pair $[\boldsymbol{A}(t), \boldsymbol{B}(t)]$ is stabilizable.

3) Denote $\tilde{\boldsymbol{A}} \equiv \boldsymbol{A}(t) - \boldsymbol{B}(t)\boldsymbol{D}^T(t)\boldsymbol{C}(t)$ and $\tilde{\boldsymbol{C}} \equiv \boldsymbol{D}_\perp^T(t)\boldsymbol{C}(t)$, such that no unit-modulus characteristic multipliers of $\tilde{\boldsymbol{A}}(t)$ are $[\tilde{\boldsymbol{A}}(t), \tilde{\boldsymbol{C}}(t)]$ unobservable.

Assumption 1 is technical. It states that $\boldsymbol{D}^T(t)\boldsymbol{D}(t) = \boldsymbol{E}$ and $\boldsymbol{D}(t)\boldsymbol{D}^T(t) + \boldsymbol{D}_\perp(t)\boldsymbol{D}_\perp^T(t) = \boldsymbol{E}$, where $\boldsymbol{E}$ is the identity matrix of a suitable dimension. Assumption 2 is equivalent to a claim that the pair $[\tilde{\boldsymbol{A}}(t), \boldsymbol{B}(t)]$ is stabilizable. Assumption 2 together with assumption 3 assures that the periodic Riccati equation (9) has a stabilizing symmetric periodic solution.

Let $\boldsymbol{P}(t)$ be a stabilizing periodic solution of the Riccati equation (9). If a periodic feedback gain is defined as

$$\boldsymbol{F}(t) = -[\boldsymbol{B}^T(t)\boldsymbol{P}(t) + \boldsymbol{D}^T(t)\boldsymbol{C}(t)] \tag{11}$$

then the closed-loop system $\boldsymbol{A}_F(t) \equiv \boldsymbol{A}(t) + \boldsymbol{B}(t)\boldsymbol{F}(t)$ is stable, and it minimizes the L_2 norm of the signal $\boldsymbol{z}(t)$

$$\min_{\boldsymbol{u}\in L_2[0,\infty)} \|\boldsymbol{z}(t)\|_2^2 = \boldsymbol{x}^T(t_0)\boldsymbol{P}(t_0)\boldsymbol{x}(t_0) \tag{12}$$

To prove this claim denote $\boldsymbol{C}_F(t) = \boldsymbol{C}(t) + \boldsymbol{D}(t)\boldsymbol{F}(t)$. Then the Riccati equation (9) can be rearranged into a Lyapunov equation

$$-\dot{\boldsymbol{P}}(t) = \boldsymbol{P}(t)\boldsymbol{A}_F(t) + \boldsymbol{A}_F^T(t)\boldsymbol{P}(t) + \boldsymbol{C}_F^T(t)\boldsymbol{C}_F(t) \tag{13}$$

After the change of the variable $\boldsymbol{v}(t) = \boldsymbol{u}(t) - \boldsymbol{F}(t)\boldsymbol{x}(t)$, the system (10) can be rewritten as

$$\dot{\boldsymbol{x}}(t) = \boldsymbol{A}_F(t)\boldsymbol{x}(t) + \boldsymbol{B}(t)\boldsymbol{u}(t), \qquad \boldsymbol{z}(t) = \boldsymbol{C}_F(t)\boldsymbol{x}(t) + \boldsymbol{D}(t)\boldsymbol{v}(t) \tag{14}$$

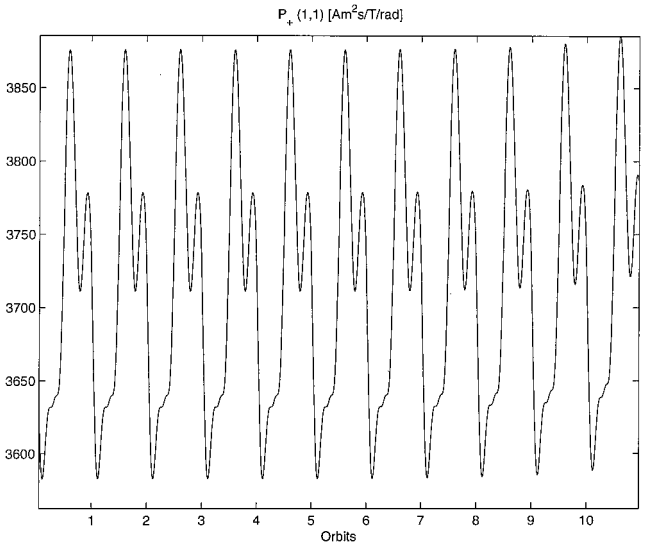

Fig. 3 Time history of the (1, 1) component of P_+; note that P_+ has a period equivalent to the orbit period.

Now define the following quadratic function $l(t) = \boldsymbol{x}^T(t)\boldsymbol{P}(t)\boldsymbol{x}(t)$ and calculate its time derivative

$$\begin{aligned}\frac{\mathrm{d}}{\mathrm{d}t}l &= \dot{\boldsymbol{x}}^T\boldsymbol{P}\boldsymbol{x} + \boldsymbol{x}^T\boldsymbol{P}\dot{\boldsymbol{x}} + \boldsymbol{x}^T\dot{\boldsymbol{P}}\boldsymbol{x} \\ &= \boldsymbol{x}^T\boldsymbol{A}_F^T\boldsymbol{P}\boldsymbol{x} + \boldsymbol{x}^T\boldsymbol{P}\boldsymbol{A}_F\boldsymbol{x} + 2\boldsymbol{x}^T\boldsymbol{P}\boldsymbol{B}\boldsymbol{v} + \boldsymbol{x}^T\dot{\boldsymbol{P}}\boldsymbol{x} \\ &= -\boldsymbol{z}^T\boldsymbol{z} + \boldsymbol{v}^T\boldsymbol{v} \end{aligned} \tag{15}$$

Both sides of Eq. (15) are integrated from 0 to ∞ and the definition of the L_2 norm is used to get the following formula:

$$\|z(t)\|_2^2 = \boldsymbol{x}^T(t_0)\boldsymbol{P}(t_0)\boldsymbol{x}(t_0) + \|v(t)\|_2^2 \tag{16}$$

Clearly the optimal control is given for $\boldsymbol{v}(t) = \boldsymbol{0}$ and $\boldsymbol{u}(t) = \boldsymbol{F}(t)\boldsymbol{x}(t)$.

At this point, one has to compute a periodic solution of the Riccati equation (9). Under controllability and observability assumptions, all solutions of the periodic Riccati equation with a positive-definite final condition converge to the unique symmetric, periodic, and positive-definite solution $\boldsymbol{P}_+(t)$. The periodic solution of the Riccati equation $\boldsymbol{P}_+(t)$ is computed from the periodic extension of the steady state solution $\boldsymbol{P}_\infty(t)$

$$\hat{\boldsymbol{P}}(t) = \begin{cases} \boldsymbol{P}_\infty(t) & \text{if} \quad 0 \le t < T \\ 0 & \text{otherwise} \end{cases} \tag{17}$$

$$\boldsymbol{P}_+(t) = \sum_{k=0}^{\infty} \hat{\boldsymbol{P}}(t - kT) \tag{18}$$

The solution $\boldsymbol{P}_\infty(t)$ is calculated using backward integration of the Riccati equation for an arbitrary positive-definite final condition. The matrix function $\boldsymbol{P}_\infty(t)$ corresponding to one orbital passage is stored in the computer's memory and then used for the subsequent orbits.

An example of the periodic matrix function $\boldsymbol{P}_+(t)$ is illustrated in Fig. 3. $\boldsymbol{P}_+(t_0)$ at fixed time t_0 is a 6×6 positive-definite matrix. Figure 3 depicts the time history of $P_+(1, 1)$, which is typical for the diagonal components. Off-diagonal components change their amplitudes between positive and negative values.

Again, the mean anomaly M can be used for parameterization of $\boldsymbol{P}_+(M)$ because both $\boldsymbol{P}_+(t)$ and $M(t)$ are T periodic. Furthermore, the controller gain matrix is also T periodic and parameterized by $\boldsymbol{M}$

$$\boldsymbol{F}_+(M) = -[\boldsymbol{B}(M)\boldsymbol{P}_+(M) + \boldsymbol{D}^T(M)\boldsymbol{C}(M)] \tag{19}$$

Implementation

The mean anomaly dependent control gain matrix $\boldsymbol{F}_+(M)$ is computed off-line and stored in the computer's memory. The control signal $\tilde{\boldsymbol{m}}(t)$ is then calculated according to

$$\tilde{\boldsymbol{m}}(t) = \boldsymbol{F}_+(M(t)) \begin{pmatrix} \boldsymbol{\Omega}_{SR}(t) \\ \boldsymbol{q}(t) \end{pmatrix} \tag{20}$$

where $\boldsymbol{\Omega}_{SR}$ is the angular velocity of the satellite relative to RCS and $\boldsymbol{q}(t)$ is the vector part of ${}^S_R\boldsymbol{q}(t)$. Finally, the magnetic moment $\boldsymbol{m}(t)$ is

$$\boldsymbol{m}(t) = \tilde{\boldsymbol{m}}(t) \times \boldsymbol{b}_{\mathrm{av}}(M(t)) \tag{21}$$

In the simulation study of the matrix $\boldsymbol{D}$, Eq. (14) has been chosen time independent

$$\boldsymbol{D} = \frac{\sqrt{2}}{2}\begin{pmatrix} \tilde{\boldsymbol{D}} \\ \tilde{\boldsymbol{D}} \end{pmatrix}, \quad \text{where } \tilde{\boldsymbol{D}} = \exp\begin{bmatrix} 0 & 1 & -1 \\ -1 & 0 & 1 \\ 1 & -1 & 0 \end{bmatrix} \tag{22}$$

which guarantees assumption 1 and keeps the velocity and attitude control effort on the same level. The choice of the matrix $\boldsymbol{C}$ is a typical tradeoff problem between good steady-state performance for large values of $\boldsymbol{C}$ and robust stability for small $\boldsymbol{C}$. Furthermore, too large a value of $\boldsymbol{C}$ excites the nonlinear terms of the satellite dynamics. The matrix $\boldsymbol{C}$ chosen in the simulation study is

$$\boldsymbol{C} = \begin{pmatrix} 100\boldsymbol{E} & \boldsymbol{0} \\ 0 & \boldsymbol{E} \end{pmatrix} \tag{23}$$

where the number 100 is introduced to make the amplitudes of the angular velocity and the vector part of the unit quaternion comparable.

Simulation results of the infinite horizon attitude control are presented in Figs. 4 and 5. Initial values of the attitude are the same in both examples corresponding to 10-deg pitch, −15-deg roll, and −30-deg yaw. Figure 4 illustrates performance of the attitude controller for the Ørsted satellite in a circular orbit. The disturbance torques are not added in this example. In Fig. 5, the Ørsted satellite is simulated in its elliptic orbit. The initial attitude is the same as in Fig. 4. The satellite motion is affected by a moderate aerodynamic drag torque corresponding to normal solar activity. The aerodynamic drag is equal 0.9×10^{-5} Nm at perigee. The attitude error is 3 deg of pitch, whereas yaw angle varies within 6 deg.

The geomagnetic field exhibits only approximately periodic nature; therefore, it is desirable to update the control parameters every second day during the entire satellite's lifetime. An alternative approach is to design a finite horizon controller such that the control parameters are updated for every orbit. This type of a control law is discussed in the next section.

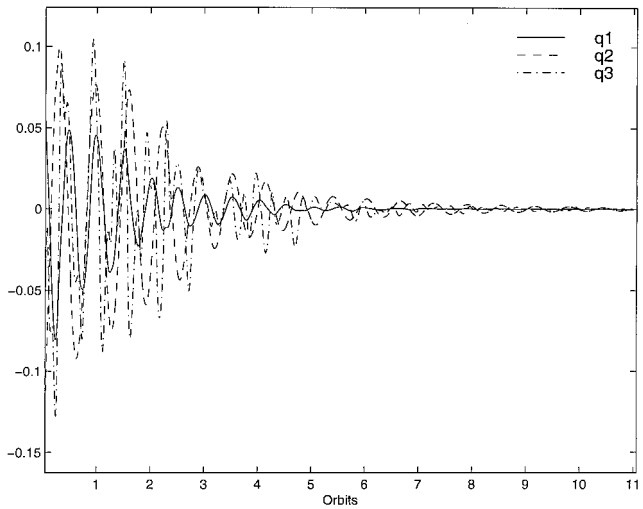

Fig. 4 Performance of infinite horizon controller for Ørsted satellite on circular orbit without disturbance torques: initial attitude is 10-deg pitch, − 15-deg roll, and − 30-deg yaw.

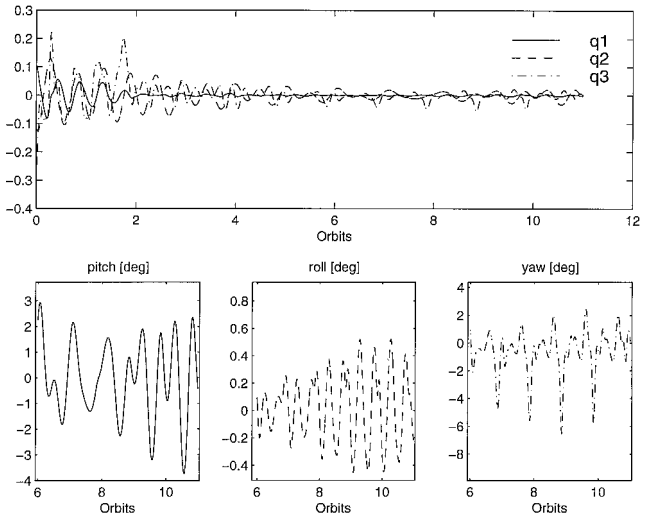

Fig. 5 Performance of the infinite horizon controller for the Ørsted satellite on its elliptic orbit.

Finite Horizon Periodic Controller

The linearized model of the satellite motion is only approximately periodic. There is a certain difference between the ideal periodic model of the geomagnetic field developed in the previous section and the real magnetic field of the Earth (Fig. 2). The controller performance could be improved by incorporating the time history of the real geomagnetic field into the controller structure. A new attitude controller based on a transient solution of the Riccati equation is therefore investigated.

The control algorithm is summarized as procedure 1, as follows:

1) Calculate the time-varying solution of the Riccati differential equation in the time interval $t \in (\tau - T, \tau]$

$$-\dot{\boldsymbol{P}}(t) = \boldsymbol{P}(t)\tilde{\boldsymbol{A}}(t) + \tilde{\boldsymbol{A}}^T(t)\boldsymbol{P}(t) - \boldsymbol{P}(t)\boldsymbol{B}(t)\boldsymbol{B}^T(t)\boldsymbol{P}(t) + \tilde{\boldsymbol{C}}^T(t)\tilde{\boldsymbol{C}}(t) \tag{24}$$

with the final condition $\boldsymbol{P}(\tau) = \boldsymbol{P}_f$.

2) Implement controller

$$\tilde{\boldsymbol{m}}(t) = -[\boldsymbol{B}^T(t)\boldsymbol{P}(t) + \boldsymbol{D}^T(t)\boldsymbol{C}(t)] \begin{pmatrix} \boldsymbol{\Omega}_{SR} \\ \boldsymbol{q} \end{pmatrix}$$

for $t \in (\tau - T, \tau]$.

3) Calculate magnetic moment from the equation $\boldsymbol{m}(t) = \tilde{\boldsymbol{m}}(t) \times \boldsymbol{b}(t)$.

4) Then τ becomes $\tau + T$.

5) Go to 1.

The important issue is the choice of the final condition $\boldsymbol{P}_f$. If the final condition is such that $\boldsymbol{H}^{(i)} = \boldsymbol{P}_f - \boldsymbol{P}(\tau - iT)$ is positive semidefinite for $i \geq 0$, then the procedure given provides a stable control law.[13]

Theorem 2: Consider a quasi-periodic system in Eq. (10). Let $[\boldsymbol{A}(t), \boldsymbol{B}(t)]$ be stabilizable and $[\boldsymbol{A}(t), \boldsymbol{C}(t)]$ observable. Let $\check{\boldsymbol{P}}(t)$ be defined as

$$\check{\boldsymbol{P}}(t) \equiv \boldsymbol{P}^{(i)}(t)$$

for $t \in (\tau + iT, \tau + (i+1)T]$ where $\boldsymbol{P}^{(i)}(t)$ is the solution to the Riccati equation (24) with the final condition $\boldsymbol{P}^{(i)}[\tau + (i+1)T] = \boldsymbol{P}_f$. Furthermore, if $\boldsymbol{H}^{(i)} \equiv \boldsymbol{P}_f - \boldsymbol{P}^{(i)}(\tau + iT)$ is positive semidefinite for every i, then the control law in procedure 1 is stable.

The attitude control system based on the final horizon control is illustrated in Fig. 6. The orbit model provides the position of the satellite in orbit in terms of longitude, latitude, and altitude. This information is used by the onboard geomagnetic field model (here the 10th-order spherical harmonic model). The Riccati equation is computed for the subsequent orbit. The controller gain is computed and parameterized by the mean anomaly. The controller gain is stored in a buffer. This procedure is repeated once per orbit. The buffer sends the control parameters to the controller on the basis of the current position of the satellite in orbit. The controller gain

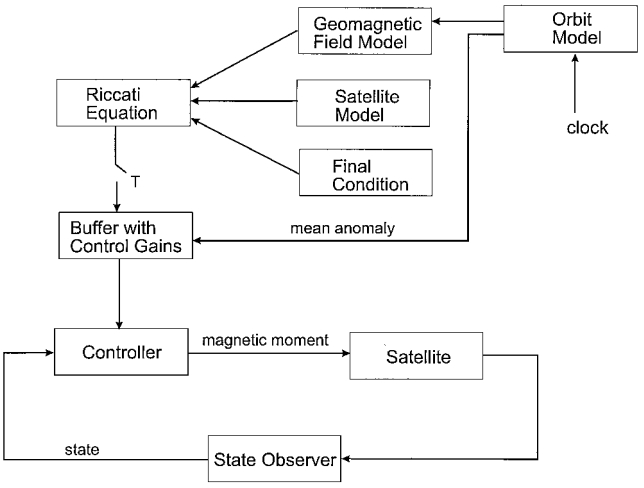

Fig. 6 Attitude control system based on finite horizon control.

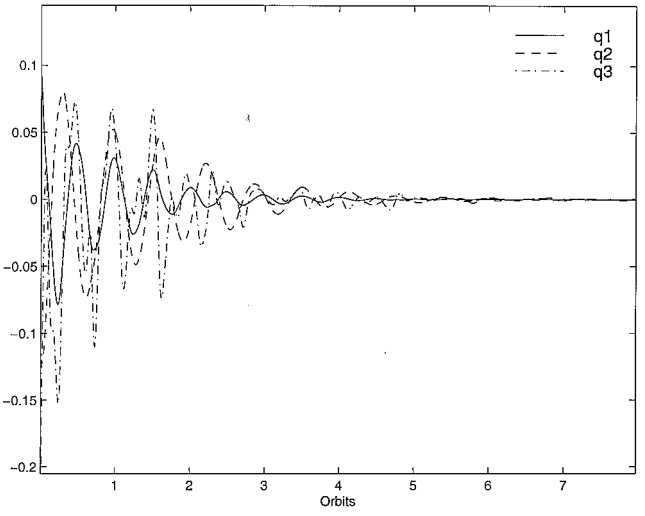

Fig. 7 Performance of the finite horizon controller for satellite on circular orbit; attitude converges asymptotically to the reference, that is, ${}^{S}_{R}\boldsymbol{q} \rightarrow [0\ 0\ 0\ 1]^T$.

is updated every sampling cycle and is implemented in the control loop.

Implementation

The simulation results for the finite horizon controller are depicted in Figs. 7 and 8. The control parameters $\boldsymbol{D}(t)$ and $\boldsymbol{C}(t)$ are the same as for the infinite horizon controller, Eqs. (22) and (23).

The final condition $\boldsymbol{P}_f$ for the finite horizon controller is chosen sufficiently large such that $\boldsymbol{H}^{(i)}$ is positive semidefinite independent of the deviation of the geomagnetic field from its periodic model. However, the larger $\boldsymbol{P}_f$ is, the larger the control torque. The controller shall comply with the power constraints imposed on the attitude control system, therefore the maximum value of the final condition shall be confined. The final condition is considered a design parameter that can be iterated by means of computer simulation. The final condition $\boldsymbol{P}_f$ for the simulation study has been calculated from the ideally periodic solution of the periodic Riccati equation (17) and (18): $\boldsymbol{P}_f = \boldsymbol{P}(\tau) = 2\boldsymbol{P}_\infty(\tau)$. The initial value of the attitude corresponds to one of the infinite horizon controllers: 10-deg pitch, −15-deg roll, and 30-deg yaw.

Figure 7 depicts the satellite motion in a circular orbit. The satellite attitude is seen to converge asymptotically to the reference. The performance of the infinite horizon controller for the satellite perturbed by the aerodynamic torque is illustrated in Fig. 8. The steady-state errors of the receding horizon and the infinite horizon attitude controller in Fig. 5 are comparable. The infinite horizon is seen to converge faster than the infinite horizon controller; however, the

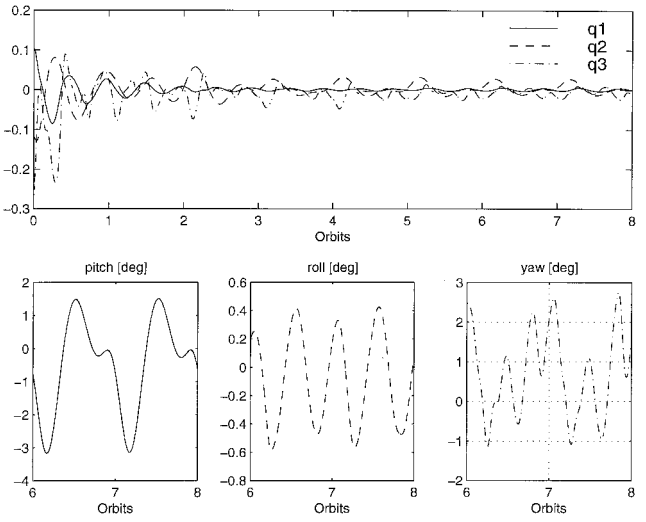

Fig. 8 Performance of the finite horizon controller for the Ørsted satellite influenced by the aerodynamic torque.

steady-state error is very much the same for both controllers when the satellite is influenced by the aerodynamic drag. Note that the aerodynamic torque is not incorporated into the linear model of the satellite motion.

The computational burden for the finite horizon controller is heavy due to the Riccati equation being solved onboard. The infinite horizon controller is preferable for the Ørsted satellite because the additional complexity of the finite horizon controller compensates for effects that are small compared to the dominant errors due to aerodynamic drag common to both controllers. The necessary computer power could be additionally limited if the constant controller was implemented and had the same performance as the time-varying controllers. This issue is addressed in the next section.

Constant Gain Control

Computation of the infinite and finite horizon attitude controllers is tedious and difficult to implement on a real-time platform. A simple constant gain attitude controller could be an alternative. The design algorithm consists of replacing the time-varying parameters of the satellite with its averaged values evaluated over a period of one orbit. This concept was used both for momentum unloading[2,8,9] and pure three-axis attitude control.[10,13] The resultant time-invariant system used for control synthesis is only an approximation of the periodic system as seen in the next subsection. Therefore, application of Floquet theory[14] is necessary for the stability check of the resultant constant gain controller.

Monodromy Matrix Approximation

Consider the closed-loop system $\boldsymbol{A}_c = \boldsymbol{A} - \boldsymbol{B}(t)\boldsymbol{F}$, with constant feedback gain $\boldsymbol{F}$. The transition matrix $\boldsymbol{\Phi}_{A_c}(t, t_0)$ of $\boldsymbol{A}_c$ evaluated within one period, that is, for $t = t_0 + T$, is named the monodromy matrix $\boldsymbol{\Psi}_{A_c}(t_0)$. Its characteristic multipliers [eigenvalues of $\boldsymbol{\Psi}_{A_c}(t_0)$] lying in the open unit disk determine the stability of a linear periodic system.[14] The following differential equation describes the time propagation of the transition matrix $\boldsymbol{\Phi}_{A_c}(t, t_0)$

$$\dot{\boldsymbol{\Phi}}_{A_c}(t, t_0) = \boldsymbol{A}_c(t)\boldsymbol{\Phi}_{A_c}(t, t_0) \tag{25}$$

with the initial condition $\boldsymbol{\Phi}_{A_c}(t_0, t_0) = \boldsymbol{I}$. An approximate solution of Eq. (25) can be given in terms of Picard's method of successive approximations (see Ref. 15):

The first approximation is

$$\boldsymbol{\Phi}^{(1)}_{A_c}(t, t_0) = \boldsymbol{I} + \int_{t_0}^{t} \boldsymbol{A}_c(t)\,\mathrm{d}t \tag{26}$$

The nth approximation is

$$\boldsymbol{\Phi}^{(n)}_{A_c}(t, t_0) = \boldsymbol{I} + \int_{t_0}^{t} \boldsymbol{A}_c(t)\boldsymbol{\Phi}^{(n-1)}_{A_c}(t, t_0)\,\mathrm{d}t \tag{27}$$

Stability of the nth-order approximation of the monodromy matrix $\boldsymbol{\Psi}^{(n)}_{A_c}(t_0)$ is implied by the stability of the following system with constant coefficients:

$$\dot{\boldsymbol{x}} = \boldsymbol{A}^{(n)}\boldsymbol{x} \tag{28}$$

where

$$\boldsymbol{A}^{(n)} = \frac{1}{T}\int_{t_0}^{t_0+T} \boldsymbol{A}_c(t)\boldsymbol{\Phi}^{(n-1)}_{A_c}(t, t_0)\,\mathrm{d}t \tag{29}$$

The eigenvalues of $\boldsymbol{A}^{(n)}$ are given by

$$\det\left(\lambda_A \boldsymbol{E} - \boldsymbol{A}^{(n)}\right) = 0 \tag{30}$$

whereas

$$\det\left(\lambda_\Psi \boldsymbol{E} - \boldsymbol{E} - T\boldsymbol{A}^{(n)}\right) = 0 \tag{31}$$

is the equation of the characteristic multipliers of the monodromy matrix $\boldsymbol{\Psi}^{(n)}_{A_c}$. Thus, from Eqs. (30) and (31),

$$\lambda_\Psi = T\lambda_A + 1 \tag{32}$$

but the monodromy matrix $\boldsymbol{\Psi}^{(n)}_{A_c}$ is stable if its characteristic multipliers satisfies $|\lambda_\Psi| < 1$, thus,

$$-(2/T) < \lambda_A < 0 \tag{33}$$

Hence, the time constants of the time invariant counterpart (28) shall be larger than $T/2$ to fulfill the stability condition for the periodic system, or, in other words, the bandwidth in all channels of the system (28) shall be less than $2/T$.

Control Synthesis

The first-order approximation of the monodromy matrix, Eq. (26), is used in this subsection for synthesis of a constant gain control law. The time-invariant counterpart of the time-varying linearized satellite motion is

$$\frac{\mathrm{d}}{\mathrm{d}t}\begin{pmatrix}\delta\boldsymbol{\Omega}\\ \delta\boldsymbol{q}\end{pmatrix} = \boldsymbol{A}\begin{pmatrix}\delta\boldsymbol{\Omega}\\ \delta\boldsymbol{q}\end{pmatrix} + \boldsymbol{B}\tilde{\boldsymbol{m}}, \qquad \boldsymbol{z} = \boldsymbol{C}\begin{pmatrix}\delta\boldsymbol{\Omega}\\ \delta\boldsymbol{q}\end{pmatrix} + \boldsymbol{D}\tilde{\boldsymbol{m}} \tag{34}$$

where

$$\boldsymbol{B} = \frac{1}{T}\int_0^T \hat{\boldsymbol{B}}[M(t)]\,\mathrm{d}t \tag{35}$$

T is the orbital period, and $\hat{\boldsymbol{B}}(M)$ is the control matrix in Eq. (8).

A linear quadratic regulator (LQR) is used for the constant gain controller design. The system is linear, time-invariant, and controllable, thus, a control law can be based on the solution of the steady-state Riccati equation.[16] The optimal control is given by

$$\tilde{\boldsymbol{m}} = -(\boldsymbol{B}^T\boldsymbol{P} + \boldsymbol{D}^T\boldsymbol{C})\begin{pmatrix}\delta\boldsymbol{\Omega}\\ \delta\boldsymbol{q}\end{pmatrix} \tag{36}$$

where $\boldsymbol{P}$ satisfies the Riccati algebraic equation

$$\boldsymbol{P}\tilde{\boldsymbol{A}} + \tilde{\boldsymbol{A}}^T\boldsymbol{P} - \boldsymbol{P}\boldsymbol{B}\boldsymbol{B}^T\boldsymbol{P} + \tilde{\boldsymbol{C}}^T\tilde{\boldsymbol{C}} = \boldsymbol{0} \tag{37}$$

Once the control vector $\tilde{\boldsymbol{m}}$ in Eq. (36) is calculated, the magnetic moment $\boldsymbol{m}$ is computed according to Eq. (2).

Stability of the control law in Eqs. (36) and (2) for the time-varying linear model of the satellite in Eq. (6) is determined using Floquet theory. This check is necessary because stability of the time-varying system and its time-invariant counterpart are not equivalent. As shown in the last subsection, the time-invariant system is only the first-order approximation of the time-varying one. Furthermore, the sensitivities of those systems are not equivalent either. For example, the disturbance torque acting on the satellite in the direction of yaw in a zone near the North or South Pole remains unaffected by the attitude controller (due to lack of controllability), whereas it can be arbitrarily damped by an LQ controller for the time-invariant counterpart.

The following closed-loop system is considered for the Floquet analysis

$$\frac{\mathrm{d}}{\mathrm{d}t}\begin{pmatrix}\delta\Omega\\ \delta q\end{pmatrix} = \{A - \hat{B}^T[M(t)]P - D^T C\}\begin{pmatrix}\delta\Omega\\ \delta q\end{pmatrix} \tag{38}$$

As seen from Eqs. (37) and (38), stability of the closed-loop system is dependent on the matrices C and D. Figure 9 depicts the locus of the characteristic multipliers for

$$C = \epsilon\begin{pmatrix}100E & 0\\ 0 & E\end{pmatrix} \tag{39}$$

where ϵ changes from 0.1 to 10 and D is the same as in Eq. (22). The satellite becomes unstable for $\epsilon = 5$. As expected for large values of ϵ, the system becomes unstable because the eigenvalues the system (34) with the feedback (36) do not obey the inequality (33).

Note that the averaged geomagnetic field is implemented for the Floquet analysis. Therefore, an ultimate test is the simulation for the nonlinear model of the satellite in the realistic space environment.

Validation

The constant gain control demonstrated stability for the entire envelope of the expected initial attitudes and angular velocities in the science observation mission phase. The control parameter, the matrices C and D, are the same as for the infinite and finite horizon controllers. The simulation result for the Ørsted satellite in a circular orbit shown in Fig. 10 shows a larger amplitude of yaw oscillations compared with the infinite and finite horizon controllers, for which the initial values are the same. Figure 11 illustrates the satellite motion on impact of the aerodynamic drag and the torque due to the eccentricity of the Ørsted orbit.

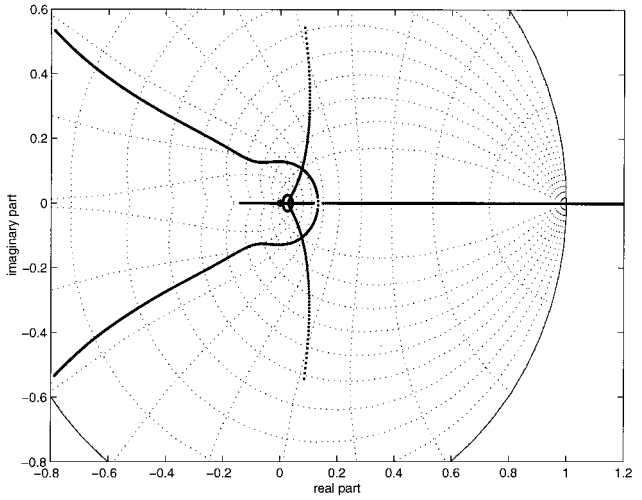

Fig. 9 Locus of the characteristic multipliers $\lambda(\epsilon)$ for ϵ changing from 0.1 to 10, evaluated for the closed-loop system in Eq. (38).

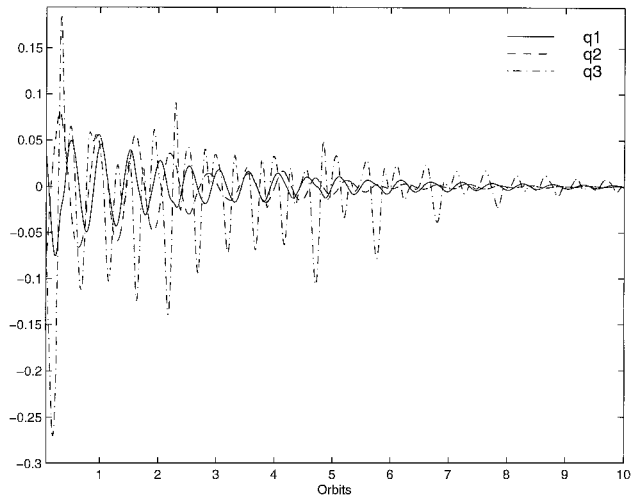

Fig. 10 Performance of constant gain controller for Ørsted satellite in circular orbit.

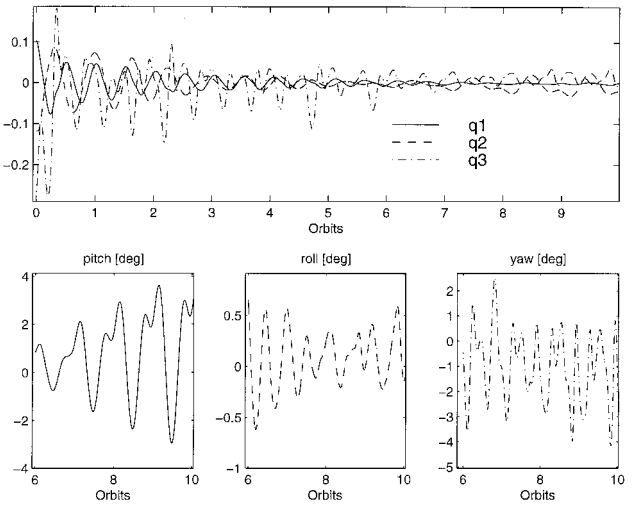

Fig. 11 Performance of constant gain controller for Ørsted satellite in elliptic orbit influenced by aerodynamic drag.

The performance of the constant gain controller is very much the same as the infinite and finite horizon attitude controllers in Figs. 5 and 8. They all have low bandwidths with time constants of the order of one orbit. The attitude error of the constant gain controller is within 4 deg, which complies with required bond of ± 10 deg of pitch, roll, and yaw. This controller was chosen for onboard implementation due to its simplicity.

Conclusions

This paper presented work on magnetic attitude control based on the steady-state and the transient solution of the Riccati equation. It was shown that a satellite in a near-polar orbit actuated by a set of perpendicular magnetorquers could be described by a set of periodic differential equations. Three attitude controllers were designed: the finite horizon, the infinite horizon, and the constant gain controller. The control strategies presented were evaluated in the simulation study.

The performance of the designed controllers was comparable for a satellite in an elliptic orbit effected by aerodynamic drag. The computer expense was smallest for the constant gain controller, therefore it was chosen for onboard implementation in the Ørsted satellite. This controller was seen to be stable for a wide envelope of initial values of the attitude, though it had inherently low bandwidth, with time constants on the order of one orbit.

This work is believed to contribute to application of the theory of periodic linear systems to magnetic attitude control problems. It provides solutions useful for small satellites with loose requirements on pointing accuracy.

Acknowledgment

The support of this work by the Danish Ørsted Satellite Project and by the Faculty of Technology and Science at Aalborg University is greatly appreciated.

References

[1]Bak, T., Wisniewski, R., and Blanke, M., "Autonomous Attitude Determination and Control System for the Ørsted Satellite," *IEEE Aerospace Applications Conference*, IEEE Publ., Piscataway, NJ, 1996, pp. 173–186.

[2]Camillo, P., and Markley, F., "Orbit-Averaged Behavior of Magnetic Control Laws for Momentum Unloading," *Journal of Guidance and Control*, Vol. 3, No. 6, 1980, pp. 563–568.

[3]Cavallo, A., Maria, G. D., Ferrara, F., and Nistri, P., "A Sliding Manifold Approach to Satellite Attitude Control," *12th World Congress IFAC*, Elsevier,

Oxford, 1993, pp. 177–184.
[4]Wisniewski, R., "Nonlinear Control for Satellite Detumbling Based on Magnetic Torquing," *Joint Services Data Exchange for Guidance, Navigation, and Control*, Draper Lab., Cambridge, MA, 1994, p. 10A.
[5]Steyn, W., "Comparison of Low-Earth-Orbiting Satellite Attitude Controllers Submitted to Controllability Constraints," *Journal of Guidance, Control, and Dynamics*, Vol. 17, No. 4, 1994, pp. 795–804.
[6]Wisniewski, R., and Blanke, M., "Three-Axis Satellite Attitude Control Based on Magnetic Torquing," *13th IFAC World Congress*, Elsevier, Oxford, 1996, pp. 291–297.
[7]Arduini, C., and Baiocco, P., "Active Magnetic Damping Attitude Control for Gravity Gradient Stabilized Spacecraft," *Journal of Guidance, Control, and Dynamics*, Vol. 20, No. 1, 1997, pp. 117–122.
[8]Hablani, H., "Comparative Stability Analyses and Performance of Magnetic Controllers for Momentum Bias Satellites," *Journal of Guidance, Control, and Dynamics*, Vol. 18, No. 6, 1995, pp. 1313–1320.
[9]Hablani, H., "Pole-Placement Technique for Magnetic Momentum Removal of Earth-Pointing Spacecraft," *Journal of Guidance, Control, and Dynamics*, Vol. 20, No. 2, 1997, pp. 268–275.
[10]Martel, F., Parimal, K., and Psiaki, M., "Active Magnetic Control System for Gravity Gradient Stabilized Spacecraft," *Annual AIAA/Utah State University Conference on Small Satellites*, AIAA, Washington, DC, 1988, pp. 1–10.
[11]Wertz, J. (ed.), *Spacecraft Attitude Determination and Control*, Kluwer Academic, Norwell, MA, 1990, pp. 414–416.
[12]Bittanti, S., Laub, A., and Willems, J. C. (eds.), *The Riccati Equation*, Springer–Verlag, Berlin, 1991, pp. 127–162.
[13]Wisniewski, R., *Satellite Attitude Control Using Only Electromagnetic Actuation*, Ph.D. Thesis, Dept. of Control Engineering, Aalborg Univ., Aalborg, Denmark, Dec. 1996, pp. 87–114.
[14]Mohler, R., *Nonlinear Systems*, Dynamics and Control, Vol. 1, Prentice–Hall, Upper Saddle River, NJ, 1991, pp. 105–114.
[15]Hille, E., *Ordinary Differential Equations in the Complex Domain*, Wiley, New York, 1976, pp. 47–51.
[16]Zhou, K., Doyle, J., and Glover, K., *Robust and Optimal Control*, Prentice–Hall, Upper Saddle River, NJ, 1996, pp. 373–381.